Title	Effect of Locally Applied Fluvastatin in Low-turnover Osteoporosis Model Mouse with Femur Bone Defect
Author(s) Alternative	Ohira, T; Tanabe, K; Sasaki, H; Yoshinari, M; Yajima, Y
Journal	Journal of Hard Tissue Biology, 24(2): 147-154
URL	http://hdl.handle.net/10130/3929
Right	

Journal of Hard Tissue Biology 24[2] (2015) 147- 154

CODEN-JHTBFF, ISSN 1341-7649

Original

Effect of Locally Applied Fluvastatin in Low-turnover Osteoporosis Model Mouse with Femur Bone Defect

Takashi Ohira[1,2], Koji Tanabe[2,3], Hodaka Sasaki[1,2], Masao Yoshinari[2] and Yasutomo Yajima[1,2]

[1] *Department of Oral and Maxillofacial Implantology, Tokyo Dental College, Tokyo, Japan*
[2] *Division of Oral Implants Research, Oral Health Science Center, Tokyo Dental College, Tokyo, Japan*
[3] *Department of Pharmacology, Tokyo Dental College, Tokyo, Japan*
(Accepted for publication, February 16, 2015)

Abstract: The aim of this study was to investigate the effects of local administration of fluvastatin-gelatin complex on the healing of bone defects in low-turnover osteoporosis mice. Gelatin was used as a carrier of the fluvastatin. A fluvastatin-gelatin complex solution was created by dissolving each concentration of fluvastatin in a 75mg/mL gelatin solution. The gelatin solution was mixed with air, then lyophilized for 1 day and cross-linked by dry heating to make a fluvastatin-gelatin complex sponge. After crosslinking, the complex sponge was cut into pieces 1 mm diameter × 1 mm high to fit the bone defect area. The amount of fluvastatin in the sponge was adjusted to control (0 nmol), 0.1 nmol, 0.2 nmol, and 0.4 nmol. Using 20-week-old low-turnover osteoporosis model mice (SAMP6) and normal model mice (SAMR1), cylindrical and bone defects were made in sites 1.0 mm in diameter and depth, 1 mm of 3 mm from both sides of the distal end of the femur. The complex sponge was then inserted into each site, and the wound was closed. Radiographic analysis and histologic examinations were then performed. In SAMP6, the bone volumes of the bone defect areas in the 0.1nmol and 0.2nmol groups were significantly higher compared with those of the control and 0.4nmol groups at 14 and 21 days. Histological observation showed that the volume of newly formed bone increased in the 0.1nmol and 0.2nmol groups compared to those in the control and 0.4nmol groups at 14 and 21 days. The bone volumes of newly formed bone in SAMR1 were higher than were those in SAMP6, and the optimum concentration of fluvastatin was different between SAMP6 and SAMR1. The present study suggests that local administration of a fluvastatin-gelatin complex sponge provides improvement in bone healing in low-turnover osteoporosis.

Key words: Fluvastatin-gelatin complex, Low-turnover osteoporosis, Local-administration, Bone formation, Micro-CT

Introduction

One of the well-known risk factors of prognosis for dental implants is osteoporosis, which has two types, high-turnover osteoporosis and low-turnover osteoporosis[1]. Many studies on low-turnover osteoporosis have used the senescence-accelerated mouse prone 6 (SAMP6) strain of mice, a type that develops low-turnover osteoporosis[2]. In particular, low-turnover osteoporosis has been reported to decrease the density of both cortical bone and trabecular bone and peri-implant bone[3]. Accordingly, investigation of low-turnover osteoporosis is considered to be important for dental implant treatment all of elderly people.

Statins are competitive inhibitors of 3-hydroxy-2-methyl-glutaryl coenzyme A (HMG-CoA) reductase, and are widely used to lower cholesterol levels, which is an important factor in the treatment of hyperlipidemia and arteriosclerosis[4]. Recently, another in vivo effect of statins has also attracted attention, with a number of studies finding that statins promote the differentiation of osteoblasts produced by stimulation with bone morphogenetic protein-2 (BMP-2), indicating their potential in the development of new osteogenic drugs[5-8].

However, the high dose of systemic administration of statins presents a serious problem with risks such as rhabdomyolysis[9,10]. Accordingly, the local administration may be recommended for enhancing the bone formation in jawbone[8]. Previous experiments by our group have shown that local administration of fluvastatin, one of the statins, promotes osteogenesis in normal rat bone defect models using a fluvastatin-gelatin complex[11,12]. In our previous study, influence of the local administration of fluvastatin on bone healing was evaluated in a senile osteoporosis model rat[13]. However, no study was reported about the local administration of statins on bone healing using low-turnover osteoporosis model mice.

In this study, the effect of local administration of fluvastatin on bone healing in low-turnover osteoporosis model mice and senescence-accelerated mouse resistant mice as a normal model

Correspondence to: Dr. Takashi Ohira, Department of Oral Maxillofacial and Implantology, Tokyo Dental College, 2-9-18 Misakicho, Chiyoda-ku, Tokyo, 101-0061 Japan; Tel: +81-3-3262-9257 Fax: +81-3-6380-9349; E-mail: oohiratakashi@tdc.ac.jp

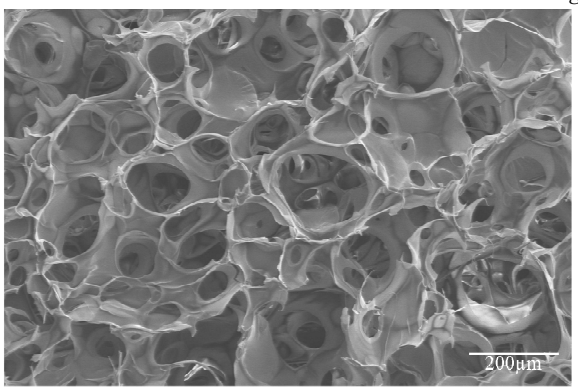

Figure 1. SEM image of gelatin sponge. SEM image of the sponge with its porous structure with pore diameters of approximately 200 μm

was evaluated radiologically and histologically using a fluvastatin-gelatin complex. The overall objective of this study was to investigate the effects of the local administration of fluvastatin on the healing of bone defects in low-turnover osteoporosis.

Materials and Methods

Preparation of fluvastatin-gelatin complex sponge

An alkaline gelatin (isoelectric point of 7.0–9.0, Nitta Gelatin, Osaka, Japan) and fluvastatin sodium salt (Toronto Research Chemicals Inc., Ontario, Canada) were used in this study.

The gelatin was dissolved in ultra-pure water to make a 75 mg/mL gelatin solution, and then the fluvastatin was dissolved in the gelatin solution to make a fluvastatin-gelatin complex solution. Subsequently, one syringe containing 1 ml of the fluvastatin-gelatin complex solution was connected with another syringe with 2 ml of air using a syringe connector, and the solutions were foamed by an emulsion preparation method similar to making an adjuvant emulsion[14].

The solutions were successively lyophilized for 1 day, and then cross-linked by dry heating (125 °C, 30 min) to make fluvastatin-gelatin complex sponge. After crosslinking, the complex sponge was cut into pieces 1.0 mm in diameter and height to fit the bone defect area. The amount of fluvastatin in a sponge was adjusted to 0.1 nmol, 0.2 nmol, and 0.4 nmol. A gelatin sponge without fluvastatin (0 nmol) was used as a control.

Fig. 1 is a SEM image of the sponge with its porous structure with pore diameters of approximately 200 μm.

Animal experiment

Twenty-week-old male senescence-accelerated mouse resistant (SAMR1) mice (Japan SLC Inc., Shizuoka, Japan) were used as a control. SAMP6 mice (Japan SLC Inc., Shizuoka, Japan) were used as models of low-turnover osteoporosis. Both groups were allowed food and water ad libitum and maintained on a 12-h light/dark cycle (lights on from 8:00 to 20:00) at 23±1 °C with 60±10 % humidity during the experiment. Both groups were anesthetized by intraperitoneal injection (60 mg/kg body weight) of sodium pentobarbital (Somnopentyl, Kyoritsu Seiyaku Co. Ltd., Tokyo, Japan).

The overlying skin of the femur was shaved and disinfected with iodated alcohol. The outside skin from the central femur to the knee was incised longitudinally, and the muscles were split to expose the femur, preserving the sciatic nerve.

A 1.0 mm round bur was used to create a cylindrical bone defect with 1.0 mm in diameter and depth under constant irrigation with normal saline solution to prevent overheating of the bone edges. The bone defect was carefully created 3 mm from the femoral distal epiphysis while avoiding any damage to the growth plate (Fig. 2 a). Cortical bone perforation was confirmed by bleeding from the bone marrow. The complex sponge, selected randomly was then inserted into each site. After inserted the complex sponge, the muscle and skin were sutured. The experimental protocol is shown in Fig. 2 b.

All animals survived and recovered quickly from surgery. The mice appeared to be in good health throughout the test periods. All animal experiments in this study were conducted in accordance with the Tokyo Dental College Guidelines for Animal Experiments (Approval date: 4/1/2013; Approval number: 253005).

Radiological analysis of chronological change in bone formation

X-ray micro-CT images were taken using an in vivo 3D micro X-ray CT System R_mCT (Rigaku Co., Tokyo, Japan). Micro-CT images were obtained from each mouse immediately after (0 day) and at 7, 14, and 21 days after bone defect creation under inhalation anesthesia with isoflurane. The samples were set on the object stage and imaging was performed over a full 360-degree rotation with an exposure time of 2 min. The conditions for Micro-CT were as follows: tube voltage, 85 kV; tube current, 160 mA; magnification, 10×; and slice width, 20 μm.

Representative images for calculating the bone volume (BV) each day on an identical animal are shown in Fig. 3. Micro-CT images were taken from the identical animal at 0 day, 7, 14, and 21 days (Fig. 3 a), after which they were merged using TRI/3D-Bon software (Ratoc System Engineering Co. Ltd., Tokyo, Japan) with a TRI/3D-Adj optional feature (Ratoc System Engineering Co. Ltd., Tokyo, Japan) (Fig. 3 b). Chronological changes at 7, 14, and 21 days were calculated by subtracting the 0 day value from each day's measurement (Fig. 3 c). A cylindrical region of interest (ROI) with 1.0mm in diameter and height of the femur was selected for analysis. The ROI was placed where the original defect was located, as the margins were visually recognizable. Mask work was performed to binarize the 3-D data set in the ROI. Finally, bone volume (BV, mm^3) with new bone was measured directly.

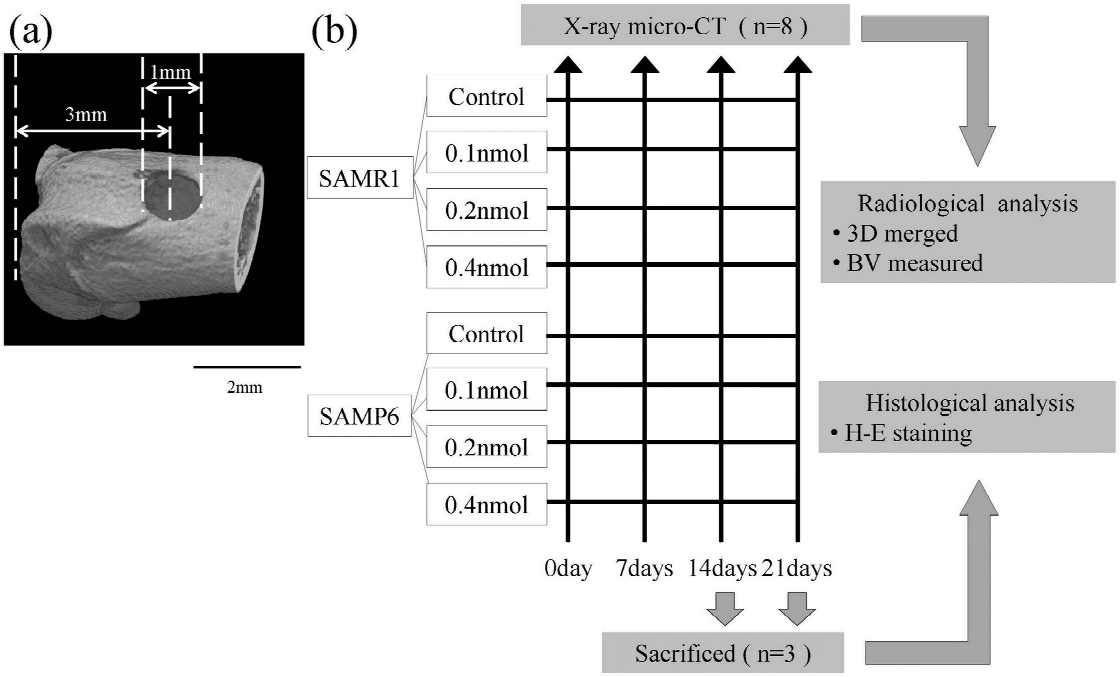

Figure 2. Bone defect model in mouse femur (a) and experimental protocol (b).

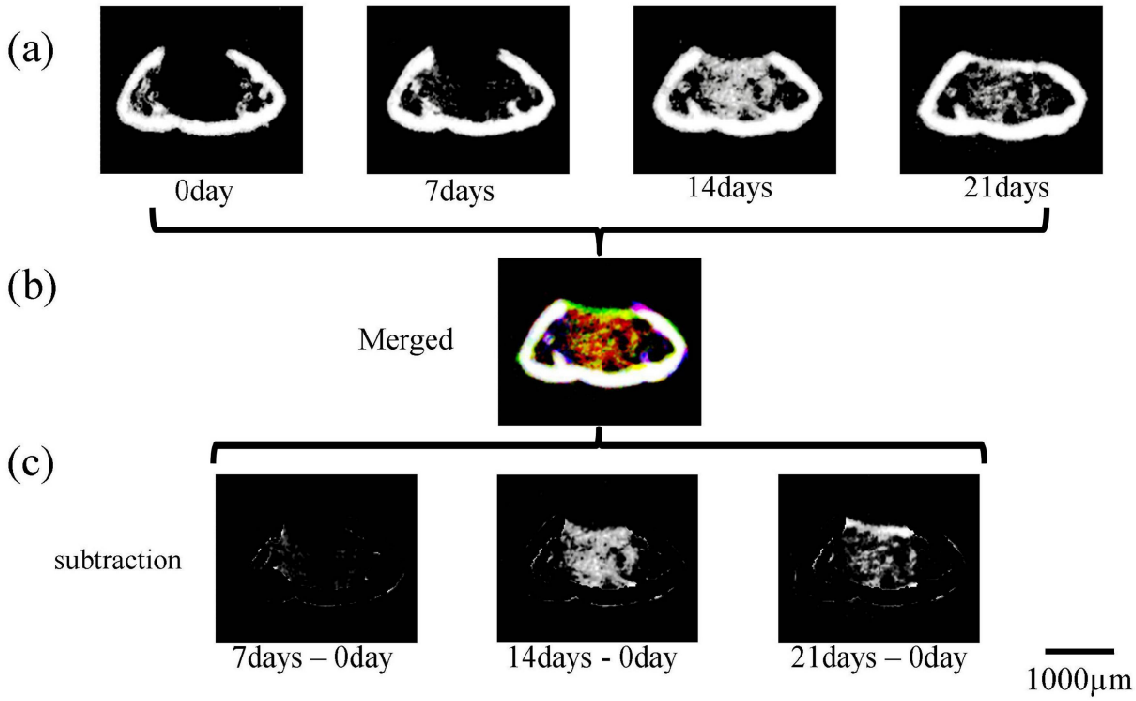

Figure 3. Representative X-ray micro-CT images for calculating the bon volume (BV) at each day on an identical animal. (a): Micro-CT images at 0day, 7, 14 and 21days; (b): Merged images with three colors: 7 day; blue, 14 days; red, 21 days; green; (c): Subtracted images 0 day from each days;

Histological analysis

Two mice were randomly selected in each groups, and euthanized on days 14 and 21 after surgery. The femur area including the bone defect was extirpated. The femurs were fixed in 10 % neutral buffered formalin at 4 ºC for 1 day and decalcified with EDTA (pH 7.0-7.5; Wako Pure Chemical Industries, Osaka, Japan) for 5 days. Paraffin sections 3 μm thick were prepared and stained with hematoxylin-eosin (H-E) according to the standard procedure. Histological observation was performed using a universal microscope (Axiophot 2, Carl Zeiss, Oberkochen, Germany).

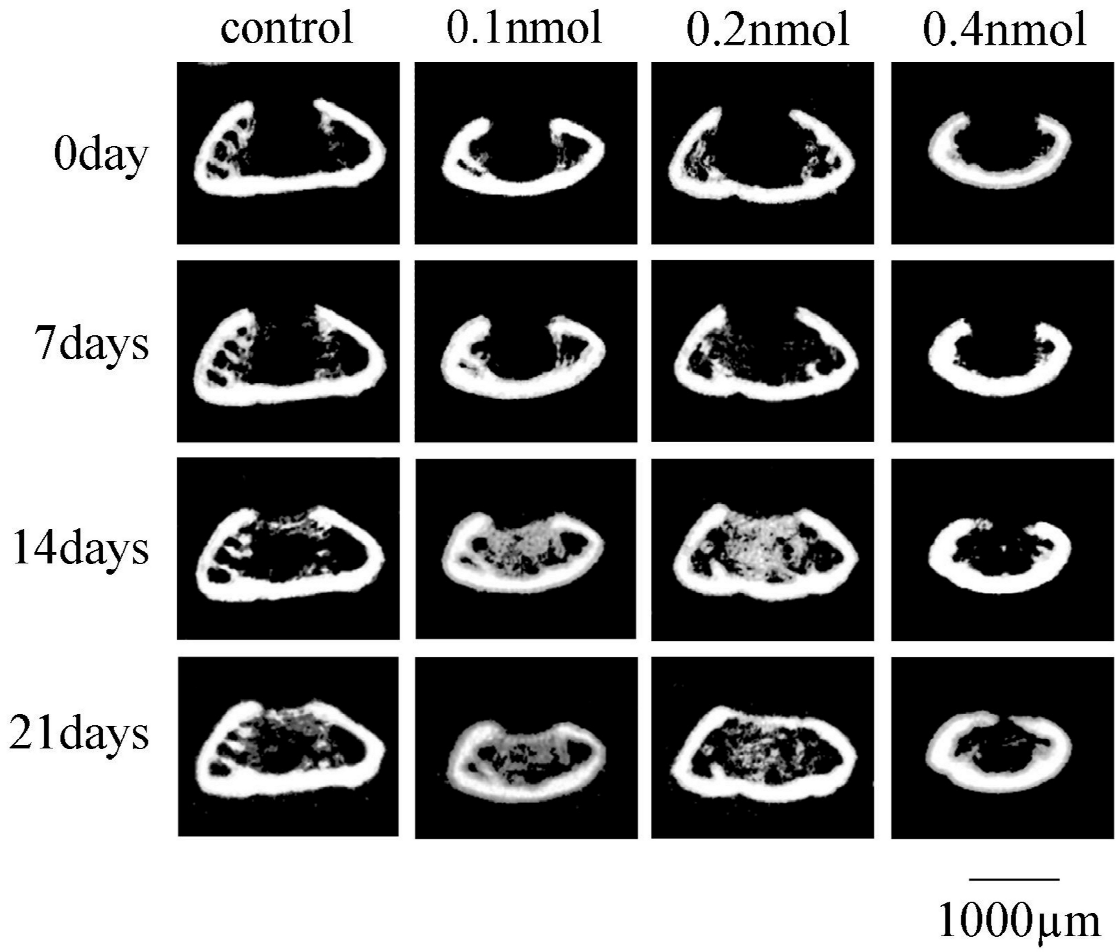

Figure 4A. Representative micro-CT images of bone defect area at days 0, 7, 14, 21 in SAMR1. At 7 days, newly formed bone was hardly observed in the bone defect areas of all groups.At 14 and 21 days, newly formed bone was observed in all groups, and the amount of newly formed bone in the 0.1 nmol and 0.2 nmol groups increased relative to that in the control and 0.4 nmol groups.

Statistical analysis

The data were analyzed using a statistical analysis software package (IBM SPSS Statistics 20, IBM Co., Somers, NY, USA). The BV values were analyzed using two-way analysis of variance (ANOVA) with the animal species and the amounts of fluvastatin as factors. Subsequently, Tukey's HSD multiple comparisons were performed between the amounts of fluvastatin.

Results

Radiological analysis of chronological change in bone formation

Representative micro CT images of SAMR1 at 0, 7, 14, and 21 days are shown in Fig. 4 A. At 7 days, newly formed bone was hardly observed in the bone defect areas of all groups. At 14 and 21 days, newly formed bone was observed in all groups, and the amount of newly formed bone in the 0.1 nmol and 0.2 nmol groups increased relative to that in the control and 0.4 nmol groups.

Representative micro CT images of SAMP6 at 0, 7, 14, and 21 days are shown in Fig. 4 B. At 7 days, newly formed bone was not recognized in the bone defect areas of all groups. At 14 and 21 days, newly formed bone was observed in all groups. The amount of newly formed bone increased in the 0.1 nmol and 0.2 nmol groups relative to that in the control and 0.4 nmol groups. In a comparison of SAMR1 with SAMP6, the cortical bone in SAMP6 was thinner than that of SAMR1. More newly formed bone was observed in SAMR1 than in SAMP6.

Fig. 5 shows the chronological changes in BV with new bone at 7, 14, and 21 days. The BV values of newly formed bone in SAMR1 were higher than were those in SAMP6 ($P<0.05$).

In SAMR1, the 0.1 nmol and 0.2 nmol groups yielded significantly higher BV than did the control group at 14 and 21 days. In contrast, no significant difference was observed between the control and 0.4 nmol groups. BV increased over time, and almost reached a peak at 14 days in all groups.

In SAMP6, the 0.1 nmol and 0.2 nmol groups showed significantly higher BV than did the control group at 14 and 21 days. In contrast, no significant difference was observed between the control and 0.4 nmol groups. At 21 days, the 0.1 nmol group showed significantly higher BV than did all other groups. BV almost reached a peak at 21 days in the control, 0.1 nmol, and 0.2

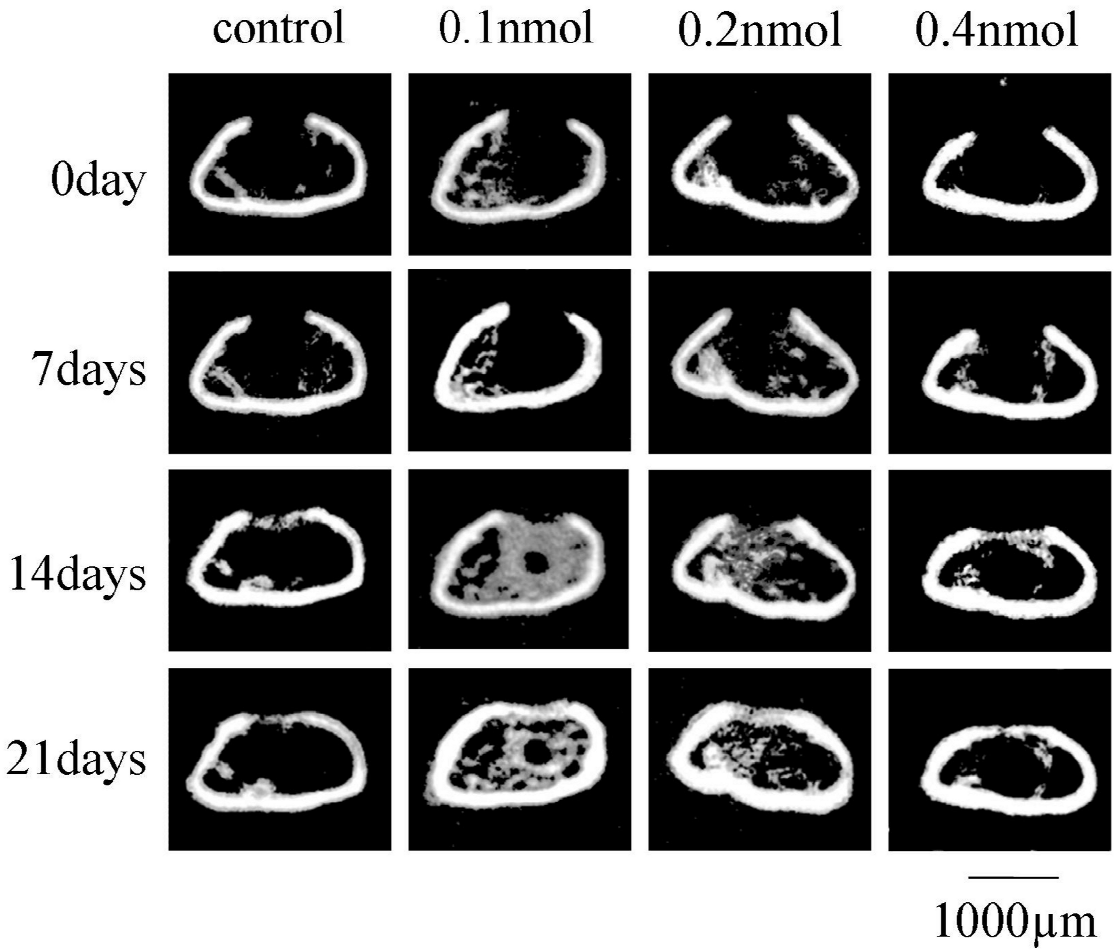

Figure 4B. Representative micro-CT images of bone defect area at days 0, 7, 14, 21 in SAMP6. At 7 days, newly formed bone was not recognized in the bone defect areas of all groups. At 14 and 21 days, newly formed bone was observed in all groups. The amount of newly formed bone increased in the 0.1 nmol and 0.2 nmol groups relative to that in the control and 0.4 nmol groups.

nmol groups.

Histological analysis

Fig. 6 shows the results of histological observation of the newly formed bone in SAMR1. At day 14, woven bone was formed in the bone defect area (Fig. 6 a-d). Woven bone of the control and 0.4 nmol groups was observed in cortical bone area (Fig. 6 a, d). On the other hand, in the 0.1 nmol and 0.2 nmol groups, woven bone was observed not only in cortical bone area but also in trabecular bone area (Fig. 6 b, c). At day 21, newly formed bone has matured in cortical bone area (Fig. 6 e-h). In addition, newly formed bone had a trabecular bone-like structure under cortical bone-like structure in the 0.1 nmol and 0.2 nmol groups, (Fig. 6 f, g)

Fig. 7 shows the results of histological observation of the newly formed bone in SAMP6. At day 14, woven bone was formed in the bone defect area (Fig. 7 a-d). Woven bone of the control and 0.4 nmol groups was observed in cortical bone area (Fig. 7a, d). On the other hand, in the 0.1 nmol and 0.2 nmol groups, woven bone was observed in not only cortical bone area but also trabecular bone area (Fig. 7 b, c). At day 21, newly formed bone had matured in cortical bone area (Fig. 7 e-h). In addition, newly formed bone had a trabecular bone-like structure under cortical bone-like structure in the 0.1 nmol and 0.2 nmol groups same as SAMR1(Fig. 7 f, g).

In a comparison of SAMR1 with SAMP6, trabecular bone-like structure of SAMP6 was thinner than that of SAMR1.

Discussion

In this study, using a fluvastatin-gelatin complex sponge, the effect of local administration on bone healing of low-turnover osteoporosis model mice was evaluated. The results showed that improved bone healing was recognized in the low-turnover osteoporosis model. Similar results were reported in our previous study showing that the osteogenic effect of fluvastatin was extended by using a fluvastatin-gelatin complex in senile osteoporosis model rats[13].

The release characteristics of fluvastatin from the fluvastatin-gelatin complex sponge were investigated in previous studies[15,16]. The results showed that the rate of dissolution of a gelatin sponge

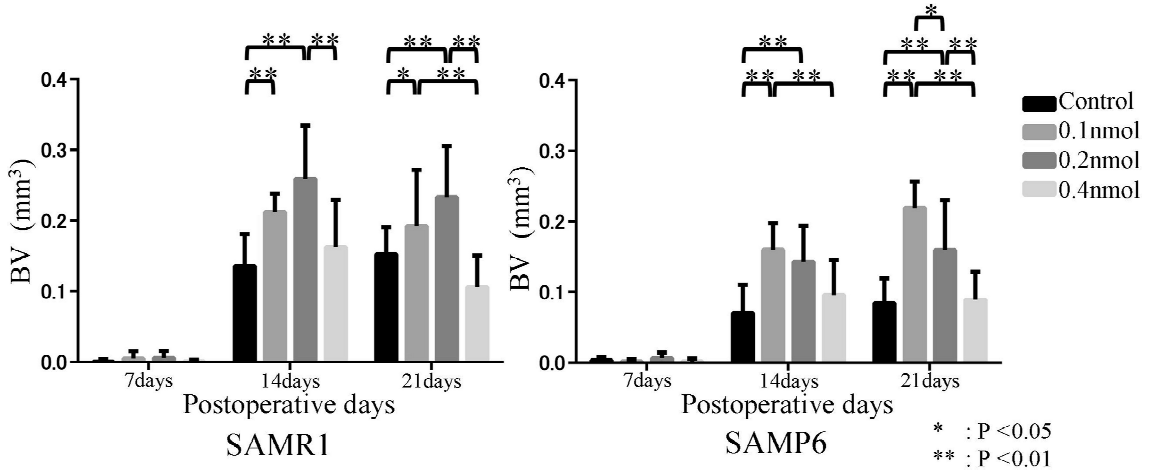

Figure 5. BV valuesin SAMR1 and SAMP6 at 7 days, 14 days, and 21 days.

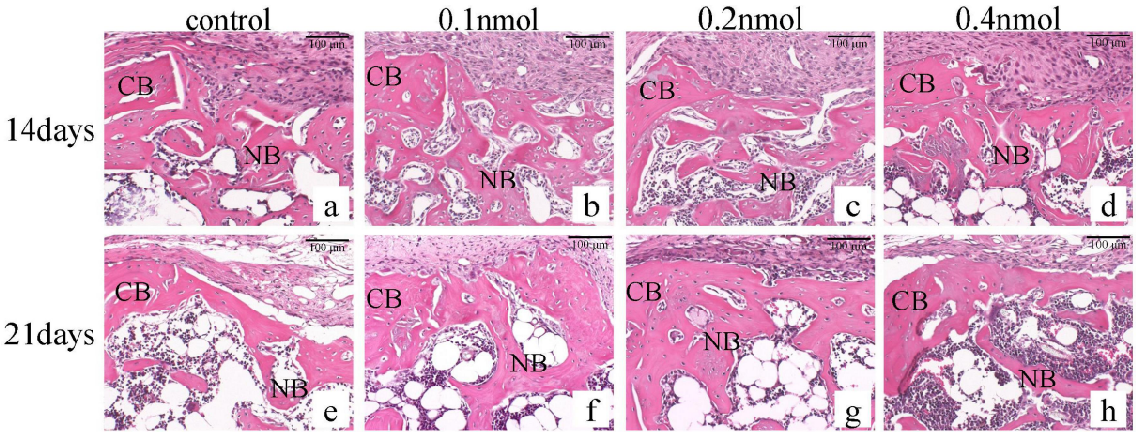

Figure 6. Histological observation of bone healing process in SAMR1 (CB: cortical bone; NB: new bone). At day 14, woven bone was formed in the bone defect area (a-d). Woven bone of control and 0.4 nmol groups was observed in cortical bone area (a, d). On the other hand, in 0.1 nmol and 0.2 nmol groups, woven bone was observed in not only cortical bone area but also trabecular bone area (b, c). At day 21, newly formed bone has matured in cortical bone area (e-h). In addition, newly formed bone had a trabecular bone-like structure under cortical bone-like structure in 0.1 nmol and 0.2 nmol groups, (f, g).

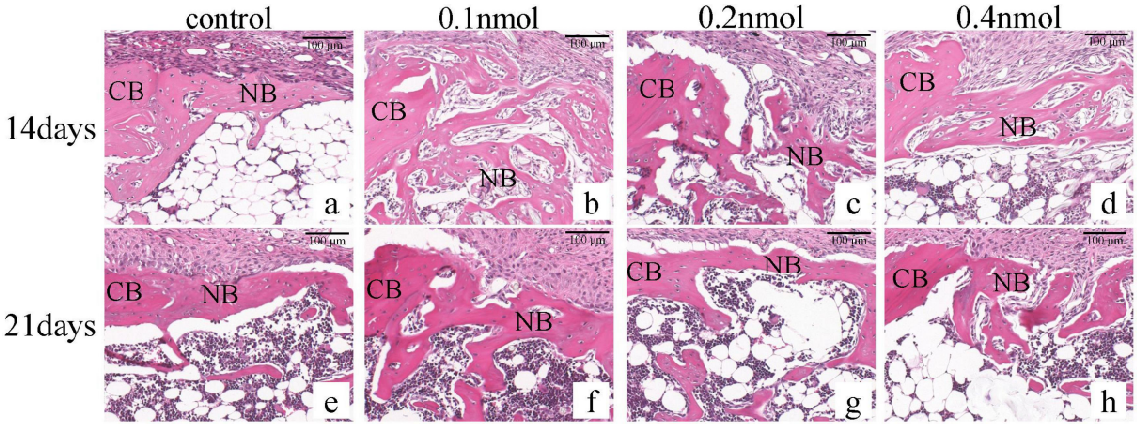

Figure 7 .Histological observation of bone healing process in SAMP6 (CB: cortical bone; NB: new bone). At day 14, woven bone was formed in the bone defect area (a-d). Woven bone of control and 0.4 nmol groups was observed in cortical bone area (a, d). On the other hand, in 0.1 nmol and 0.2 nmol groups, woven bone was observed in not only cortical bone area but also trabecular bone area (b, c). At day 21, newly formed bone newly formed bone have matured in cortical bone area (e-h). In addition, newly formed bone had a trabecular bone-like structure under cortical bone-like structure in 0.1 nmol and 0.2 nmol groups same as SAMR1 (f, g).

is controllable by changing the rate of thermal cross-linking. Accordingly, the time of dissolution of the gelatin could be extended by controlling the rate of thermal cross-linking over three days. In addition, since the fluvastatin and gelatin were combined electrically, fluvastatin is believed to be released gradually with the dissolving gelatin. Indeed, the wide-range degradation of the fluvastatin-gelatin complex sponge was recognized in the bone defect areas in this study. These results suggest that the release of fluvastatin occurred gradually and that the released fluvastatin may have pharmaceutical efficacy for bone healing. Another advantage of the fluvastatin-gelatin complex sponge is easy handling, leading to convenience in clinical applications.

In this study, fluvastatin was used to investigate the effect of the local administration of statins. Hydrophobic statins (simvastatin, lovastatin) enter the liver via the hepatic portal vein, while hydrophilic statins (rosuvastatin, pravastatin, fluvastatin) require active transport into the cell[17]. Simvastatin is administered by gavage and requires hepatic conversion to metabolically active β-hydroxy acid to become medicinally active. Therefore, for local administration, simvastatin must first be hydrolyzed to form simvastatin acid[18,19]. The structure of fluvastatin is significantly different from those of previously used HMG-CoA reductase inhibitors such as the pravastatin and simvastatin metabolites, which are derived from fungi[20,21]. Therefore, it was considered that fluvastatin might have a pharmacological effect on bone formation in addition to the main effect of HMG-CoA reductase inhibitory activity. Some authors reported the positive effect of locally applied fluvastatin on bone[6,11,12]. However, the mechanisms of the osteogenic effect of fluvastatin are not entirely clear.

Significant increases of BV as well as newly formed bone in histological observation were recognized in the 0.1 nmol and 0.2 nmol groups at 14 and 21 days using micro-CT analysis of SAMR1 in this study. In the 0.4 nmol group, however, the amount of new bone formation was lower than was that in the 0.1 nmol and 0.2 nmol groups for 21 days. This result indicates that high-dose fluvastatin inhibits bone healing. Several studies have reported that a high dose of simvastatin inhibits bone healing because of the induction of inflammation[22,23]. These high-dose-induced inflammations were suggested as inhibiting bone healing. Our results agreed with these reports.

The cortical bone in SAMP6 used in this study was thinner than that of SAMR1 on the micro-CT images. That attribute is considered to be caused by the mouse species, that is, the thin cortical bone in SAMP6 represents a typical feature of the SAMP6 mouse. Furthermore, BV in SAMP6 were lower than were those in SAMR1 in this study. This result is believed to be due to osteoblastic hypoplasia that inhibits the healing of bone defects[2,24].

The optimum concentration of fluvastatin was different between the SAMP6 and SAMR1 mice in this study. This may be due to the different susceptibility of the fluvastatin by SAMP6 and SAMR1. Further studies are necessary to clarify the dose-dependent effect of fluvastatin on normal and osteoporosis models in vitro. In addition, for clinical applications, it is necessary to determine the optimum doses of fluvastatin carefully.

In conclusion, the present study revealed that local administration of a fluvastatin-gelatin complex sponge improved bone healing in low-turnover osteoporosis.

Acknowledgments

This research was supported by a Grant-in-Aid for Scientific Research (B:18390524 and Young Scientists (B) 258618971) from the Japan Society for the Promotion of Science.

References

1. Alsaadi G, Quirynen M, Komárek A and Van Steenberghe D. Impact of local and systemic factors on the incidence of oral implant failures, up to abutment connection. J Clin Periodontol 34: 610-617, 2007
2. Silva MJ, Brodt MD, Fan Z and Rho J-Y. Nanoindentation and whole-bone bending estimates of material properties in bones from the senescence accelerated mouse SAMP6. J Biomech 37: 1639-1646, 2004
3. Matsushita M, Tsuboyama T, Kasai R, Okumura H, Yamamuro T, Higuchi K, Higuchi K, Kohno A, Yonezu T, Utani A, Umezawa M and Takeda T. Age-related changes in bone mass in the senescence-accelerated mouse (SAM). Am J Pathol 125: 276-283, 1986
4. Shao H, Tan Y, Eton D, Yang Z, Uberti MG, Li S, Schulick A and Yu H. Statin and stromal cell-derived factor-1 additively promote angiogenesis by enhancement of progenitor cells incorporation into new vessels. Stem Cells 26: 1376-1384, 2008
5. Mundy G, Garrett R, Harris S, Chan J, Chen D, Rossini G, Boyce B, Zhao M and Gutierrez G. Stimulation of bone formation in vitro and in rodents by statins. Science 286: 1946-1949, 1999
6. Moriyama Y, Ayukawa Y, Ogino Y, Atsuta I and Koyano K. Topical application of statin affects bone healing around implants. Clin Oral Implants Res 19: 600-605, 2008
7. Nyan M, Sato D, Kihara H, Machida T, Ohya K and Kasugai S. Effects of the combination with α-tricalcium phosphate and simvastatin on bone regeneration. Clin Oral Implants Res 20: 280-287, 2009
8. Ayukawa Y, Yasukawa E, Moriyama Y, Ogino Y, Wada H, Atsuta I and Koyano K. Local application of statin promotes bone repair through the suppression of osteoclasts and the enhancement of osteoblasts at bone-healing sites in rats. Oral Surg Oral Med Oral Pathol Oral Radiol Endod 107: 336-342, 2009
9. Hodel C. Myopathy and rhabdomyolysis with lipid-lowering

drugs. Toxicol Lett 128: 159-168, 2002

10. Ogasawara R, Furuya Y, Sasaki H, Yoshinari M and Yajima Y. Effects of oral administration of simvastatin on bone formation in senile osteoporosis rat. J Hard Tissue Biol 22: 461-472, 2013
11. Tanabe K, Nomoto H, Okumori N, Miura T and Yoshinari M. Osteogenic effect of fluvastatin combined with biodegradable gelatin-hydrogel. Dent Mater J 31: 489-493, 2012
12. Tanabe K, Saima H, Suzuki K, Miura T and Yoshinari M. Effect of fluvastatin release on local osteogenicity in rat calvaria. J Oral Tissue Eng 8: 181-187, 2011
13. Yasuda H, Tanabe K, Sato T, Nomoto S, Miura T and Yoshinari M. Osteogenic effect of local administration of fluvastatin using a fluvastatin-gelatin complex in senile osteoporosis model rat. J Hard Tissue Biol 23: 389-398, 2014
14. Freund J. Some aspects of active immunization. Annu Rev Microbiol 1: 291-308, 1947
15. Tanabe K, Miura T and Yoshinari M. Electrostatically coupled state of fluvastatin with gelatin in vitro. J Hard Tissue Biol 22: 451-454, 2013
16. Dreesmann L, Ahlers M and Schlosshauer B. The pro-angiogenic characteristics of a cross-linked gelatin matrix. Biomaterials 28: 5536-5543, 2007
17. Tsartsalis AN, Dokos C, Kaiafa GD, Tsartsalis DN, Kattamis A, Hatzitolios AI and Savopoulos CG. Statins, bone formation and osteoporosis: Hope or hype? Hormones 11: 126-139, 2012
18. Yoshinari M, Hayakawa T, Matsuzaka K, Inoue T, Oda Y, Shimono M, Ide T and Tanaka T. Oxygen plasma surface modification enhances immobilization of simvastatin acid. Biomed Res 27: 29-36, 2006
19. Yoshinari M, Matsuzaka K, Hashimoto S, Ishihara K, Inoue T, Oda Y, Ide T and Tanaka T. Controlled release of simvastatin acid using cyclodextrin inclusion system. Dent Mater J 26: 451-456, 2007
20. Plosker GL and Wagstaff AJ. Fluvastatin. Drugs 51: 433-459, 1996
21. Hamelin BA and Turgeon J. Hydrophilicity/ lipophilicity: relevance for the pharmacology and clinical effects of HMG-CoA reductase inhibitors. Trends Pharmacol Sci. 19: 26-37, 1998
22. Nyan M, Sato D, Kihara H, Machida T, Ohya K and Kasugai S. Effects of the combination with α-tricalcium phosphate and simvastatin on bone regeneration. Clin Oral Implants Res 20: 280-287, 2009
23. Stein D, Lee Y, Schmid MJ, Killpack B, Genrich MA, Narayana N, Marx DB, Cullen DM and Reinhardt RA. Local simvastatin effects on mandibular bone growth and inflammation. J Periodontol 76: 1861-1870, 2005
24. Yoshida A, Sasaki H, Furuya Y, Yoshinari M and Yajima Y. Effect of low-intensity pulsed ultrasound on bone-healing process in murine low-turnover osteoporosis model. J Hard Tissue Biol 22: 301-310, 2013